Development and Validation of a Wheel Wear and Rolling Contact Fatigue Damage Model

Adam Bevan 1)*, Paul Molyneux-Berry 1), Bridget Eickhoff 2) and Mark Burstow 3)

1) Institute of Railway Research, School of Computing and Engineering, University of Huddersfield, Huddersfield, HD1 3DH, UK
2) Rail Safety and Standards Board, UK
3) Network Rail, Rail Infrastructures Limited, UK

*a.j.bevan@hud.ac.uk

ABSTRACT

This paper summaries the development of a damage model to predict the deterioration rates of the wheel tread in terms of wear and rolling contact fatigue (RCF) damage. The model uses a description of a fleet's route diagram to characterise the duty cycle of the vehicle in terms of curve radius, cant deficiency and traction/braking performance. Using this duty cycle a large number of vehicle dynamics simulations are automatically conducted to calculate wheel-rail contact forces and predict the formation of wear and RCF damage, using a combination of the Archard and frictional energy-based ($T\gamma$) damage models.

The damage models have been validated using observation data (wear rates and maximum observed RCF damage) acquired from a range of vehicle fleets in Great Britain (GB). Results from the validation of the model are presented along with a review of the wheel turning and observation data.

A piece-wise linear regression is fitted to the wear and RCF parameters predicted from the model to determine the damage rates for each wheelset type on the vehicle. These damage rates are used within the recently developed Wheelset Management Model (WMM) to describe how the attributes of the wheel (i.e. wheel diameter, profile shape and tread damage) deteriorate over time and trigger a maintenance or renewal activity when the condition of the wheel matches a particular limiting value.

This work formed part of the rail industry research programme managed by the Rail Safety and Standards Board (RSSB), and funded by the Department for Transport, to increase the rolling stock functionality of the Vehicle Track Interaction Strategic Model (VTISM) tool.

Keywords: wheel/rail damage, wheel wear, rolling contact fatigue

1. INTRODUCTION

Management of railway vehicle wheelsets accounts for a significant proportion of rail vehicle maintenance activities and can be a key driver for determining the vehicle or bogie maintenance periodicity. Although wheelsets will have planned maintenance schedules (e.g. for wheel reprofiling), damage to the wheel surface may develop rapidly, requiring a wheelset to be taken out of service for repair or replacement at short notice. This can have an impact on a fleet's service provision as well as cost. Damage to wheelsets can also cause increased damage to vehicle and track components, leading to further cost implications. An improved understanding of the dominant wheel damage mechanisms and the rates at which they occur will therefore help to determine the optimum wheelset monitoring and maintenance regimes, thereby allowing whole life costs to be reduced.

The aim of this paper is to provide a summary of a model developed to predict wheel tread damage. An overview of the theoretical methodology adopted within the model to predict wear and rolling contract fatigue damage (RCF) damage is presented, with more detailed information included in the referenced material. The developed model uses a description of a fleet's service diagram to determine a simulation environment (accounting for the distribution of curvature, cant deficiency, traction/braking etc.) that represents the duty cycle of the vehicle. Vehicle dynamic simulations are then conducted to predict the wheel-rail contact forces on each wheel in the vehicle for each of the combination of operating conditions in the simulation environment. These forces are then post-processed to predict the level of material removal and subsequent depth of RCF damage in each situation. A weighted sum of the results is then formed, according to the distribution of each simulation environment condition in the vehicle operating diagram, to predict the wear or RCF damage which will have developed.

The results from the validation of the model are presented along with some example case studies. The paper also comments on the influence of traction, braking and route characteristics on the propensity to generate wear and RCF and the effect this may have on the resulting wheel turning periodicity.

2. REVIEW OF WHEEL DAMAGE OBSERVATIONS

Initially a review of wheel turning and observation data from a number of vehicle fleets was undertaken to determine the main drivers for wheel turning and to identify the incidence of the different wheel damage mechanisms [1]. The damage reported in the data was divided into a number of categories to represent the mechanisms observed. These included:

- *Rolling contact fatigue (RCF)* – Fatigue-related damage that is induced as a result of the repeated cyclic loading and unloading together with the additional creep forces from curving, traction and braking.
- *Thin flange* – Wear concentrated on the face of the wheel flange resulting in a reduction in flange thickness (flange wear).
- *High flange* –Wear concentrated across the tread of the wheel resulting in an increase in flange height (tread wear).
- *Tread damage* – Combination of damage mechanisms relating to issues associated with the wheel material; such as flats, ovality and cavities. Flats on the wheel surface occur due to thermal damage as a result of a wheel spin or slide. The resulting heating and rapidly cooling of the wheel material generates martensite which is very hard and brittle and, following further loading, can spall out of the wheel leaving cavities.
- *Tread rollover* – Deformation of the tread material causing a lip to develop in place of the chamfer on the field side of the wheel.
- *Parity* - Turning of wheels on a wheel lathe to obtain an acceptable diameter on all wheelsets in the vehicle or bogie.
- *Other* – This category includes wheels turned for reasons other than the damage mechanisms listed above. This includes: out-of-round wheels (i.e. wheels with a run-out in the tread) due to wheel machining issues or the presence of other tread damage and observations of poor ride or vehicle stability issues.

The incident of each of these damage mechanisms within the dataset was determined and can be seen in Figure 1. It can be seen from the breakdown of the different reasons for wheel turning shown in Figure 1 that the majority of wheels within the dataset were turned due to RCF (41%) and tread damage (26%). Although a high proportion of wheels are turned for tread wear (high flange), generally these are associated with tread braked vehicles as identified in Figure 2, which illustrates the different reasons for wheel turning on either disc or tread braked vehicles.

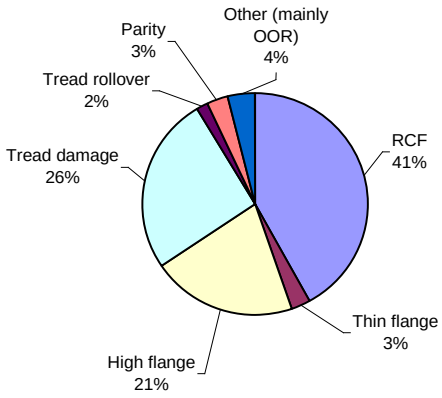

Figure 1 Overall Incidence of Wheel Damage

The aggregation of the data presented in Figure 2(b) indicates that high flange (i.e. tread wear) is reported as the major cause (76%) of wheel turning for tread braked rolling stock. For disc braked vehicles the incidence of wheels turned for wear drops dramatically, resulting in an increase in the reported incidence of RCF (50%) and tread damage (30%) modes. The reduction in RCF observed on tread braked vehicles is possibly due to the increase in wear caused by the tread brakes, which removes damaged material from the surface of the wheel before RCF becomes established. Tread braked vehicles do report a small incidence of RCF (9%), but it is possible that this is associated with thermal cracking which may appear similar to RCF.

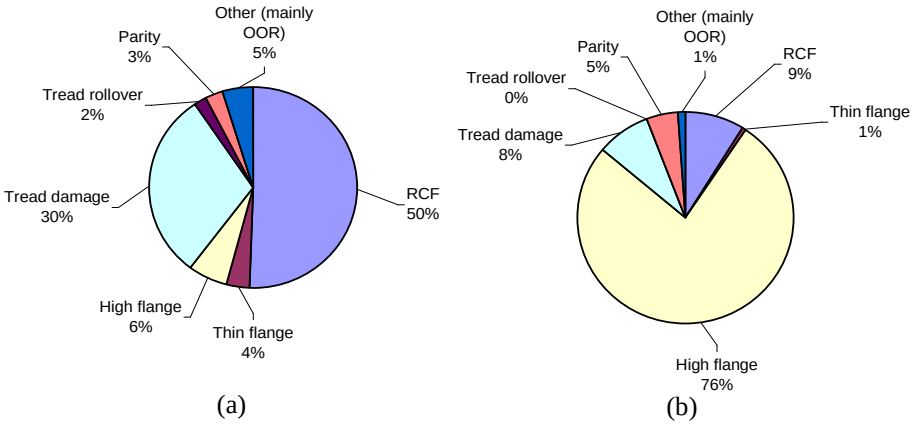

Figure 2 Incidence of Wheel Damage for (a) Disc and (b) Tread Braked Vehicles

As the majority of passenger vehicles operating on the GB rail network are disc braked, tread braked vehicles have not been considered for inclusion in the current work. Therefore the prediction of wheel wear in the model was of less importance, as illustrated in Figure 2(a) turning for wear (e.g. high or thin flange) accounts for only 10% of all wheel turning. However, the wheel profile shape can have a significant influence on the initiation and propagation of RCF damage (in both wheels and rails) and therefore worn wheel profiles are a prerequisite for

the prediction of RCF damage. They are also important when studying the effect of changes in vehicle-track characteristics on wheel wear (e.g. curve distribution, vehicle primary suspension stiffness).

The observation data obtained from a sample set of vehicles and fleets has also been used to calibrate and validate the wear and RCF models [2]. This data has been derived from visual assessment of wheel tread condition and includes a mixture of electric (EMU) and diesel multiple units (DMU) and high speed intercity trains, running on different routes and operating conditions. Investigations conducted using the observation data have highlighted the sensitivity of the model to a number of input parameters to the model including:

- Influence of traction and braking forces on the formation of RCF damage. Significant differences were apparent in the observed rates and nature of damage (e.g. crack angles) between motored and trailer axles on the same vehicle, under otherwise identical conditions. Therefore to reproduce this observation it is important to include the influence of traction and braking forces and the interaction between wear and RCF damage (wear reducing the formation of RCF damage) in the model.
- Damage rates are sensitive to the different running conditions observed by the wheel. It can be seen from both the observations and predictions that the different running conditions operated by the vehicle have a significant influence on the damage rates. A wheelset experiences a large variation of running conditions including: running in both directions, over a wide range of curve radii (including left and right hand curves) and traction and braking forces. All the damage from these different running conditions is superimposed on the wheel tread and cannot easily be related to specific route sections or running conditions. Therefore it is important to accurately describe the duty cycle of the wheelset over its service life. Work is currently on going to associate the observed damage types and locations with the vehicle running conditions that cause them [3].
- Leading axles of a train generally exhibit higher damage rates than intermediate axles. As the leading axle of a train is likely to experience higher levels of fluid contamination, the presence of fluid in the wheel-rail contact is believed to be a significant driver of crack propagation due to fluid entrapment (hydro-static pressure) [4]. Currently there is insufficient understanding to practically include this in the model.

Several theoretical models exist for a number of the different damage mechanisms [5, 6] identified within the review of wheelset turning data. These models either predict the generation of damage or the impact of the damage on wheel-rail forces. Generally, with the exception of wear and RCF, these models are not currently at a stage where they can reliably incorporated into a wheelset damage model. Therefore it was proposed to develop a model to predict the two main damage modes seen by the wheel: wear and RCF.

3. METHODOLOGY OF THE WHEEL DAMAGE MODEL

The findings from the review of wheel turning data and investigations of alternative analysis methods suggested that the wheel damage model should utilise a description of a fleet's route diagram to characterise the duty cycle of the wheelset. Using this information, a number of vehicle dynamics simulations can be conducted to represent this duty cycle and predict the wheel-rail contact forces. These forces can then be used to predict the formation of wear and RCF damage using the current available methods [7, 8]. To achieve this objective the following methodology was developed:

- Characterise a vehicle's operating conditions in terms of parameters which influence wheel damage.
- Predict wheel-rail forces for the chosen operating conditions using vehicle dynamics simulations.
- Post-process the calculated wheel-rail forces to model the formation of wear and RCF damage on the wheel using a combination of the Archard (wear) and frictional energy based (RCF) damage models. These damage models are described in more detail in Section 3.2.
- Plot and save the results for post-processing or use in strategic models such as the Vehicle Track Interaction Strategic Model (VTISM) and the Wheelset Management Model (WMM).

A schematic of the developed methodology can be seen in Figure 3. The main analysis routines, identified in italics in Figure 3, are described in more detail in the following sections.

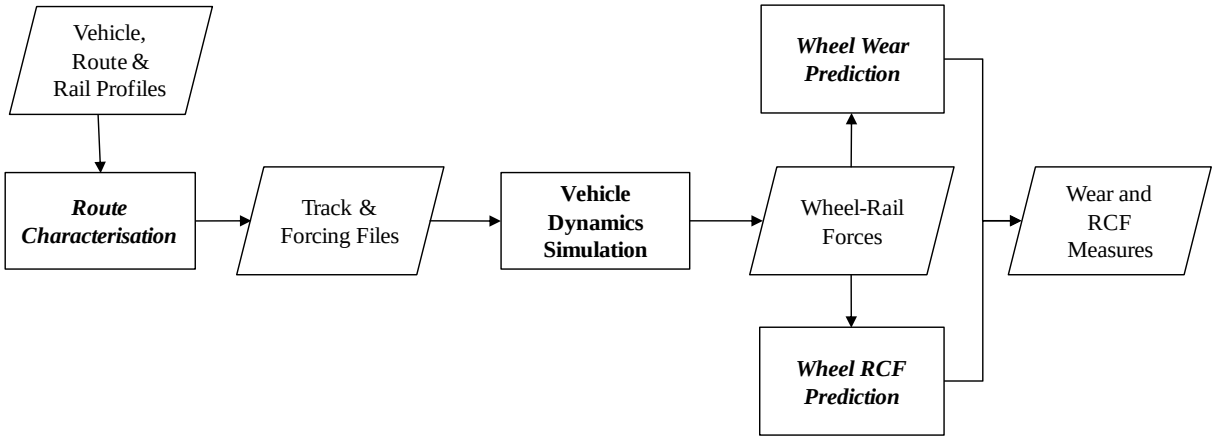

Figure 3 Methodology of the Wheel Damage Model

3.1 Route Characterisation

Generally most fleets run over a wide range of routes with a large total mileage. These routes will be made up of varying conditions (e.g. curve radius, cant deficiency, rail profiles, traction/braking forces). Running an analysis over long distances including the full range of conditions that a fleet may observe would take considerable time and require a high quality of input data. Therefore a route characterisation routine was developed to represent the duty cycle of the vehicle with a series of much shorter simulations without significantly compromising the accuracy of the results. A similar approach has been successfully applied by Jendel [9] and Enblom [10] to the prediction of wheel wear on Swedish routes.

The developed routine reads in one or more track geometry files (measured using a track recording vehicle) together with appropriate vehicle speed to represent the different route sections of a vehicles diagram. The files are then weighted to represent the frequency of operation of vehicles over these routes. The routine then selects appropriate curve radius and cant deficiency bands based on their cumulative distribution. The following approach is used to select the appropriate curve radius and cant deficiency bands (typically 6-8 curve radii per route and 2-4 cant deficiencies per radius are selected) for the analysis:

- Calculate the cumulative distribution of curves within a vehicle diagram, as shown in Figure 4(a).
- Calculate the gradient of the distribution, where a steep gradient indicates common curve radii.
- As sharp curves generally do more damage, these are prioritised by multiplying the gradient by the curvature, as shown in Figure 4(b).

- Peaks in the response are identified to determine the common curvature bands. This selection is undertaken by selecting: (1) a straight (tangent track) case and the curve with the sharpest radius, (2) curves with highest response, which are not close to previously selected radii and (3) curve radii that fill in any large gaps in the distribution. An example of this selection criterion is highlighted by the colour coded dots in Figure 4(b).
- Following the selection of appropriate curve radii the route is categorised into curvature bins and the process is repeated to select appropriate cant deficiency bins. During this process the routine ensures that the chosen vehicle speed for a particular analysis case does not exceed the maximum speed of the vehicle.

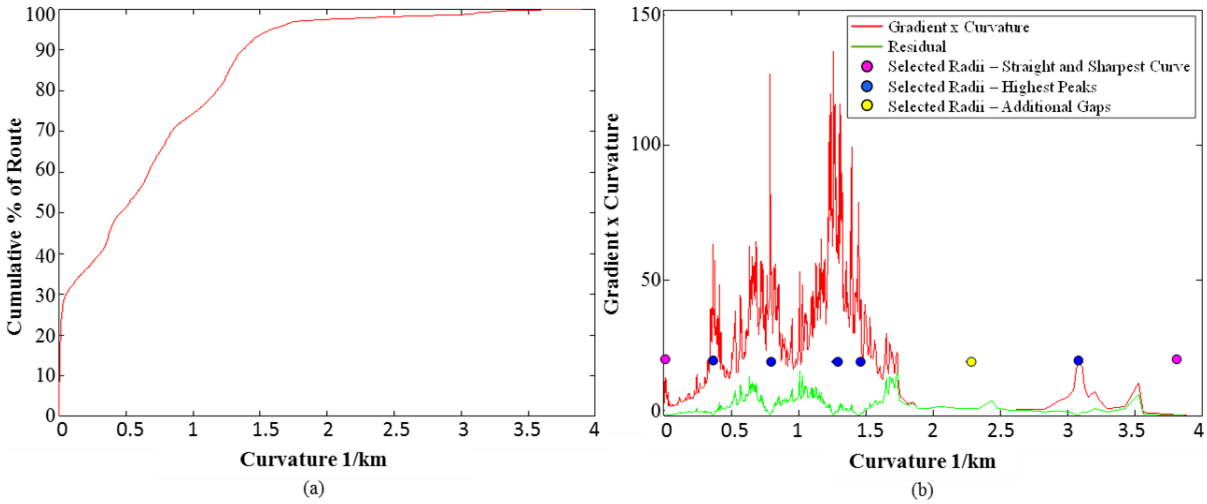

Figure 4 Route Characterisation Curve Radii Selection using (a) Cumulative Distribution of Curvature and (b) Gradient x Curvature

To allow the correct simulation of non-symmetrical routes left and right hand curves are treated separately, but vehicle dynamics simulations are only carried on one curve direction as the results can be mirrored for the opposite direction.

Sensitivity studies conducted by Jendel [11] concluded that it was sufficient to use typical track irregularities in wheel wear simulations. Therefore representative track irregularities, based on the vehicle speed and track quality band, are used in each of the selected analysis cases. This is achieved by using the standard deviation (SD), calculated from the measured lateral and vertical track irregularities (derived from track recording vehicle data) for the route, to scale the assumed track irregularities defined in the model.

As previously mentioned, it was identified from the review of fleet data that significant differences in damage rates were apparent between powered and trailer axles on the same vehicle. Therefore it would not be possible to reproduce these differences without taking into account the influence of the traction and braking forces, and the distribution of these forces through the train. Using a history of traction and barking forces for each of the different route sections of a vehicle's diagram, the route characterisation routine calculates the distribution of traction and braking forces for both powered and trailer axles. This distribution is then applied to the respective axle within the vehicle dynamics simulations.

Following the selection of appropriate curve radius, cant deficiency and traction/braking forces the routines automatically generate the input files required for the analysis. This includes:

- Track files with appropriate curvature, applied cant and vehicle speed.
- Track irregularities, selected using the vehicle speed and scaled based on the calculated standard deviation of the original route data.
- Forcing files with representative traction and braking forces for both motored and trailer axles (applied as a torque to the wheelset).
- Weighting factors to apply to each curve/cant deficiency band to represent the route characteristics.

3.2 Wheel Damage Models

Wheel-rail contact forces are predicted for the chosen route conditions using vehicle dynamics simulations. These wheel-rail forces are then post-processed to predict the formation of wear and RCF damage on the wheel using a combination of the Archard and frictional energy damage models as detailed below.

3.2.1 Prediction of Wheel Wear

It can be seen from published work that a number of computational models have been developed for the prediction of wheel wear [12]. These models generally fall in two main categories:

- Models which assume the material loss is proportional to the frictional energy dissipated in the contact patch ($T\gamma$). $T\gamma$ is expressed as the sum of the products of the creepage and creep force for the lateral, longitudinal and spin components, as illustrated below:

$$T\gamma = [T_y \gamma_y] + [T_x \gamma_x] + [M_z \omega_z]$$

  Where; T, M = Longitudinal, lateral creep force and spin creep moment components

  γ, ω = Longitudinal, lateral and spin creepage components

  A number of factors, based on the rate of the $T\gamma$, have been developed to account for the different wear regimes (e.g. mild, severe and catastrophic) [13, 14].

- Sliding models according to Archard [15], where the material loss (Vw) is proportional to the normal force (N) and the sliding distance (s) divided by the material hardness (H), as illustrated below:

$$V_w = k \frac{N \cdot s}{H}$$

  The wear coefficient (k) differs depending on the governing wear regime (e.g. mild, severe and catastrophic), properties of the wheel steel and environmental conditions as described later in this section.

The wheel damage model has utilised the wear iteration procedure previously developed by Jendel [9, 11] and Enblom [10] at the Royal Institute of Technology (KTH) and successfully applied by the first author to the prediction of wheel wear on GB rolling stock [16, 17]. This procedure is illustrated in Figure 5 and uses the Archard wear model to determine the volume of material removed and has been validated, up to high mileages, against observed wheel wear.

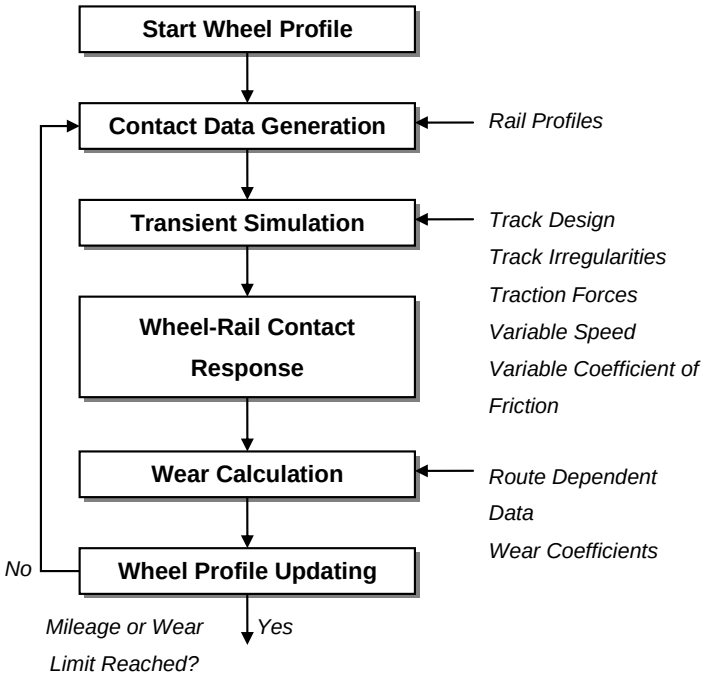

Figure 5 Methodology of Wheel Wear Prediction [7]

Although the methodology adopted by the author in [16] produced accurate results, there were a number of barriers which limited the use of these routines within a strategic model such as the WMM. The previous routines used detailed whole-route simulations and a large number of iterations to generate realistic worn wheel profile shapes. This resulted in unacceptable set-up and computational times. In order to speed up the analysis a series of shorter simulations are run, based on the definition of vehicle operating conditions developed from the route characterisation routines described in Section 3.1, and the results weighted to represent the whole-route.

The wheel-rail contact data and forces generated from the vehicle dynamic simulations are input to the wear calculation. Typical output quantities from the vehicle dynamic simulations include normal forces, size and location of the contact patch and creepages, which are used within the Archard wear model to predict the amount of material removal. These steps are combined in an automated tool which launches the VAMPIRE®[1] vehicle dynamics simulation, calculates the wear and controls the wear steps.

The volume of wear, calculated according to the Archard wear model, is multiplied by a wear coefficient (k) determined from a map of wear rates for typical wheel/rail steels. These maps have been derived from laboratory tests [19], run on twin disc and pin-on-disc machines, and field observation data by plotting the wear rate as function of the slip velocity (v_{slip}) and contact pressure (p). The wear map adopted in the work described here has been reproduced from [18] and is presented in Figure 6. A total of four wear coefficients are used to represent regions of the wear map which describe the transition between different wear regimes. These include: catastrophic (k_1), mild (k_2 and k_4) and severe wear (k_3).

The actual value of the wear coefficients has been selected, within the ranges presented in Figure 6, to represent the contact conditions and typical wheel steels used in GB by comparing the wear depth output from the model with observations of wear from a number of vehicle fleets. The majority of GB fleets operate with R8T wheel

[1] DeltaRail Group Limited, UK

steel [20], although a number of fleets have trialled alternative wheel steels designed to reduce the initiation of RCF damage and therefore additional work is required to calibrate the wear coefficients for these alternative wheel steels. Further details on the Archard wear model and wear coefficients can be found in [9, 10 and 11].

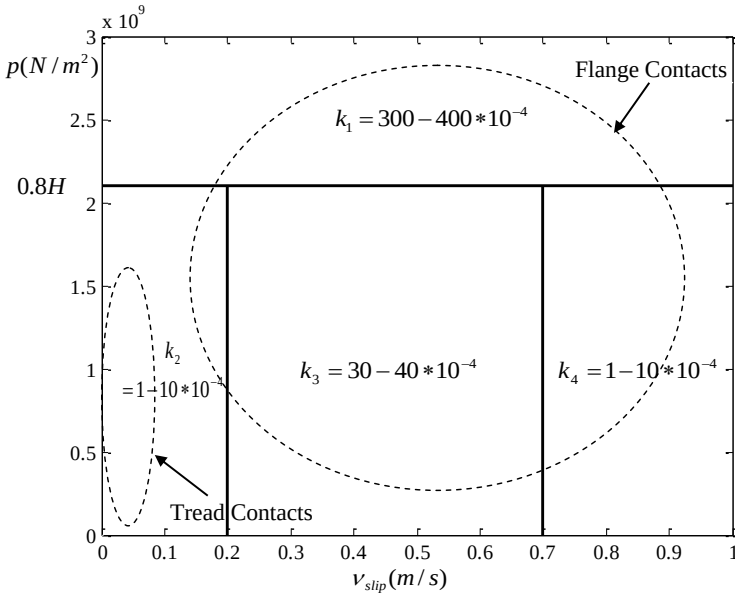

Figure 6 Wear Coefficients for Typical Tread and Flange Contacts [18]

The output from the wheel wear prediction routines includes the change in wheel profile shape with increasing running distance. Using the predicted profile shape the change in flange height (tread wear, *Sh*) and thickness (flange wear, *Sd*) with running distance are also calculated, as illustrated in Figure 7. These parameters are generally used to describe wheel profile wear and to determine wheel turning periodicity.

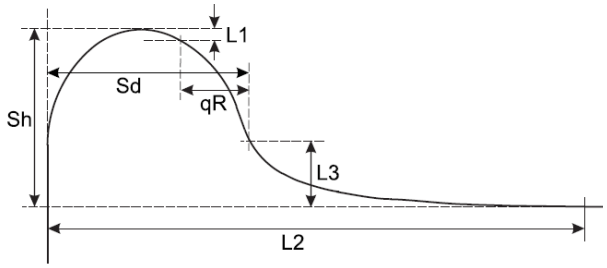

Figure 7 Definition of Wheel Wear Measures - Flange Height (*Sh*) and Flange Thickness (*Sd*)

3.2.2 Prediction of RCF Damage

Whilst several consistent and well validated wheel wear models exist, this is not true of RCF crack initiation and growth on wheels. Reviewing the available literature it can be seen that a number of methods have been trialled for the prediction of wheel RCF with varying degrees of success. These methods include:

- Shakedown theory, which states that if a contact lies above the shakedown limit then RCF (or other forms of damage) can be expected. A surface and sub-surface initiated RCF damage index has been proposed by Ekberg [21], but this method does not account for the interaction between wear and RCF generation, where an increase in the level of wear will remove RCF damage.
- Frictional energy based models, such as the Whole Life Rail Model (WLRM) [22] and the wheel RCF model developed during previous RSSB project T549 [8]. These models include the effect of wear on

the formation of RCF damage using empirically generated damage functions and have been incorporated in previous routines.

- Other models, such as finite element and brick models etc. [23]. At this stage these models are un-suitable for inclusion in a strategic tool such due to the complexity of the analysis required.

In common with models developed to predict RCF damage in rails [21], the wheel RCF prediction routine has utilised the frictional energy in the contact patch ($T\gamma$) to predict the formation of RCF cracks. A $T\gamma$-damage relationship has been developed which accounts for the interaction of wear and RCF damage, where increased levels of wear remove damage associated with RCF cracking. This relationship has been validated against observations of wheelset damage from a number of GB fleets, as illustrated in Section 4. The wheel RCF calculation process is summarised in Figure 8 and includes the following steps:

- Read outputs from the vehicle dynamics simulations conducted for each curve radius/cant deficiency band.
- Typically RCF cracks in wheels propagate more rapidly when the creep forces are in the braking direction; opening cracks in the wheel before they enter the contact patch and closing them as they come into contact with the rail (whereas rails are more sensitive to forces in the traction direction). This mechanism can accelerate crack propagation by hydrostatic pressure applied when fluid enters the crack and becomes trapped as the wheel rotates along the rail [3, 4]. To capture this mechanism the $T\gamma$ predicted for each time step is scaled based on the direction of the longitudinal creep force, such that RCF damage only occurs when the wheel is the driven surface (i.e. braking direction).
- Crack damage is calculated from the scaled $T\gamma$ and wear damage (reduction in RCF due to wear) from the raw $T\gamma$, using the developed $T\gamma$-damage relationships, and distributed elliptically over the width of the contact patch.
- The total damage per metre rolled (crack + wear damage) from each curve radius/cant deficiency band is accumulated and weighted to represent the complete vehicle operating conditions.

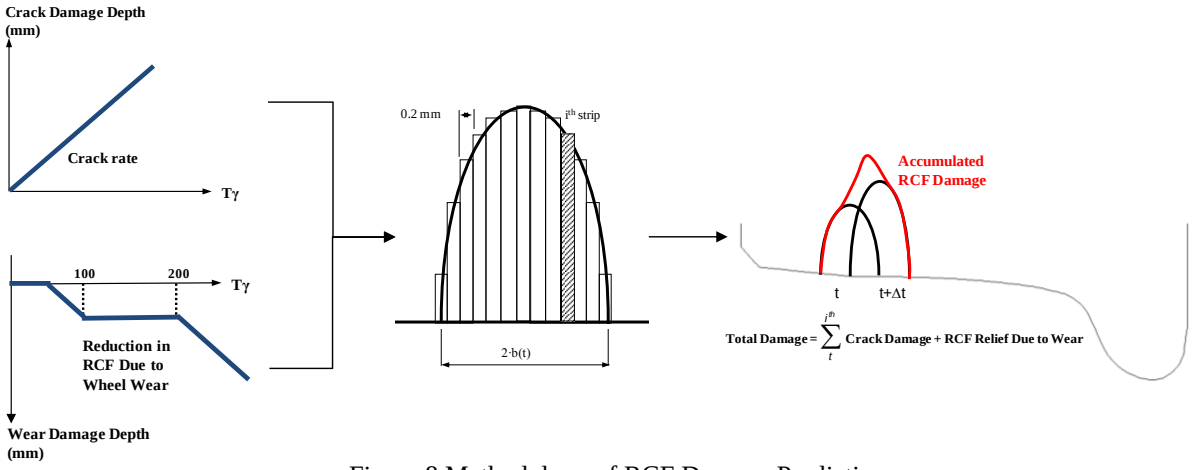

Figure 8 Methodology of RCF Damage Prediction

The distribution of damage predicted across the wheel tread is accumulated with running distance. To represent the deterioration rate of the wheel (in terms of damage rate per mile) the peak of the predicted damage distribution for different running distances is determined, as illustrated in Figure 9. The peak damage was selected as it indicates the worst damage on the wheel which could trigger a wheelset maintenance activity.

To provide an output that is directly related to strategic wheel life costs the modelled damage is reported as crack depth (mm). The depth of RCF cracks is related to the likelihood of cavities, the wheel turning interval, wheel steel properties and the actual amount of material which must be removed at turning to eliminate the damage. The ratio of crack depth to surface crack length has been determined based on the reduction in wheel diameter required to remove the observed RCF damage. Using this information it has been assumed that the crack depth is a quarter of the observed surface crack length. Future monitoring using state-of-the-art wheel crack detection equipment and the analysis of damaged wheels will help to confirm this assumption, but it is not inconsistent with the limited information available.

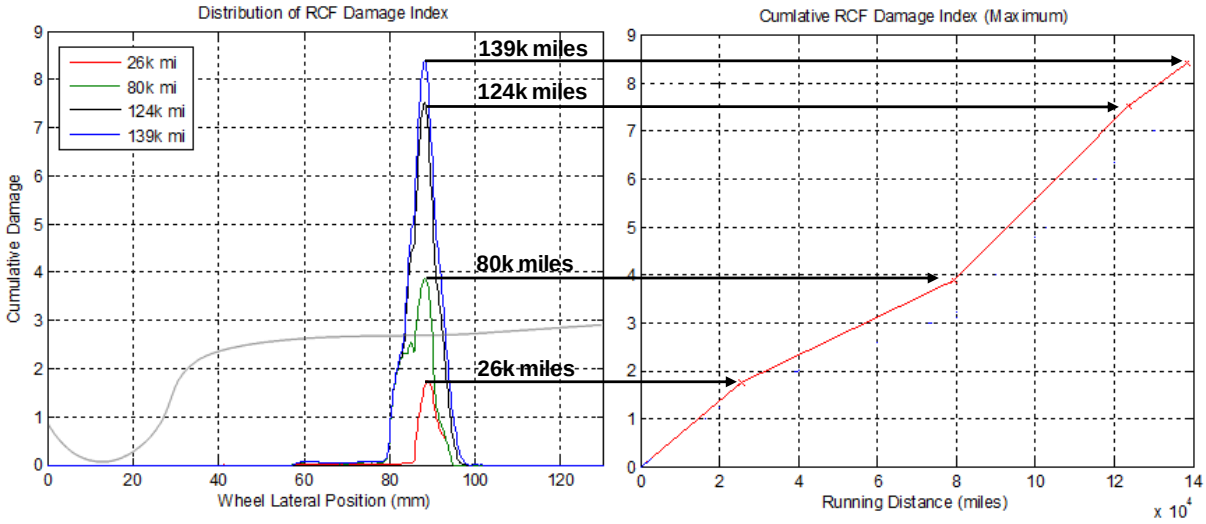

(a) (b)

Figure 9 Accumulation of Wheel RCF Damage – (a) Distribution of Damage Across the Wheel Tread and (b) Peak Damage with Running Distance

3.3 Outputs

The methodology for the prediction of wheel wear and RCF damage described above has been coded in MATLAB®[2]. The MATLAB® routine automatically runs the analysis using the VAMPIRE® vehicle dynamics simulation software and outputs both the predicted wear and RCF damage. Using these outputs the deterioration rates for each wheelset type within the vehicle are determined and help to estimate the emerging wheelset maintenance and renewal costs when used in combination within a strategic planning application, such as the recently developed WMM [24].

It can be seen from the fleet observation data that the deterioration rates of a wheel, in terms of flange wear and RCF crack growth, are generally non-linear with running distance. A piecewise linear regression has therefore been used to determine the deterioration rates of the wheel for use in the WMM. Assessment of available fleet observation data suggests that RCF cracks initially grow quickly, and then stabilise with little further growth. Therefore to capture this behaviour a two-stage regression line is fitted to the peak RCF damage data as illustrated in Figure 10.

[2] Mathworks, Inc., USA

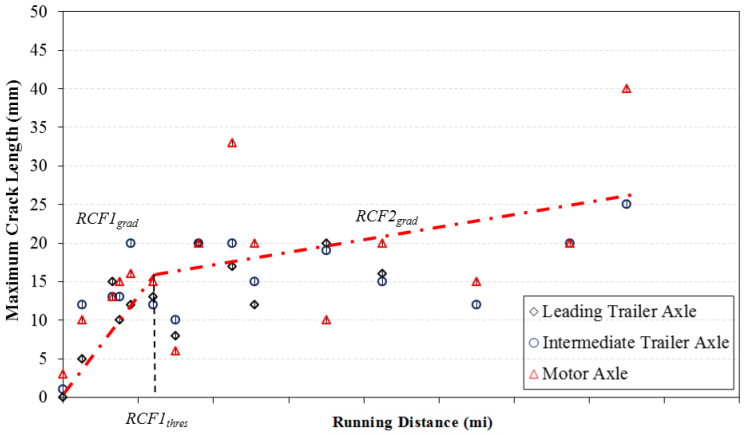

Figure 10 Wheel Tread Deterioration Rates – RCF Damage

A three-stage regression line is fitted to the predicted flange thickness (*Sd*) data, as flange wear (reduction in flange thickness, *Sd*) generally occurs early in the life of the profile and then stabilises, and in some cases is followed by an increase in flange thickness due to increasing tread wear. This behaviour is illustrated in Figure 11(b). Tread wear (increase in flange height, *Sh*) is generally linear with mileage and therefore a linear regression is fitted to the predicted flange height (*Sh*) data, as illustrated in Figure 11(a). The slope (i.e. Sd_{grad}, Sh_{grad} and RCF_{grad}) and mileage for each stage (i.e. Sh_{thres} and RCF_{thres}) are determined and reported, as illustrated in Figures 10 and 11.

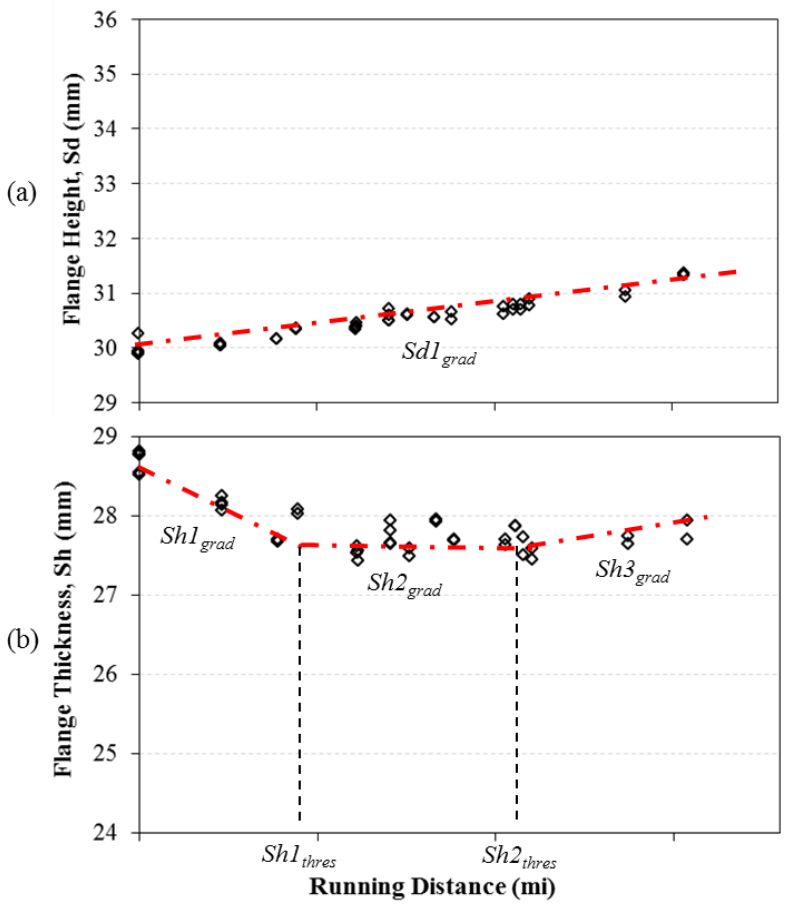

Figure 11 Wheel Tread Deterioration Rates – Tread (a) and Flange Wear (b)

4. CALIBRATION AND VALIDATION OF THE WHEEL DAMAGE MODEL

4.1 Wheel Wear

Although previous use of the wear model generated acceptable levels of the emerging wheel wear [7, 16], a number of modifications to the routines have been implemented, including the use the route characterisation approach rather than a whole-route simulation, and therefore further verification of the model was required.

The emerging wheel wear has been predicted for a typical DMU and EMU vehicle using the wheel damage model. The operating conditions of the two fleets, in terms of the routes which the vehicle operates and how frequently it operates on each of these routes, were determined and used to select appropriate track geometry for input into the model. This data was then used in the route characterisation routines to determine the duty cycle of the vehicle and prediction of wheel wear using the Archard model.

As shown in Figure 12, the modelled flange height (*Sh*) and thickness (*Sd*) have been compared to recent wheel profile measurements taken from vehicles operating similar routes. The values of flange height and thickness were calculated from these measured profiles and plotted against the respective vehicle mileage since wheel turning. It can be seen that the modelled flange height and thickness values compare reasonably well to the values observed in service for both the DMU and EMU vehicles.

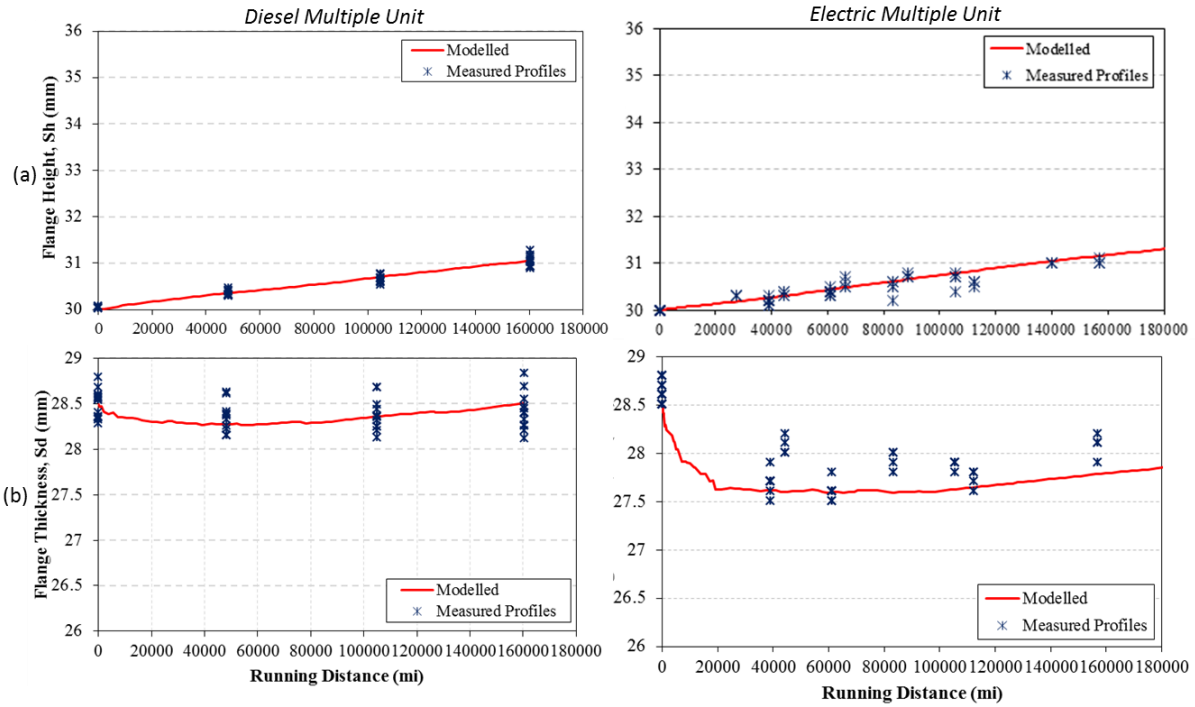

Figure 12 Modelled Flange Height (a) and Flange Thickness (b)

4.2 Rolling Contact Fatigue

The calibration of an empirical wheel RCF damage relationship is more difficult than the corresponding rail damage relationship [20], because a wheelset experiences much more varied running conditions than a length of rail. A rail is installed as either a high or low rail on a given curve radius and usually experiences fairly

consistent traffic (vehicle types, direction, speed and traction/braking). Consequently the damage mechanisms on a length of rail are fairly consistent. However, a wheel runs in both directions, experiences a wide range of curve radii (on both left and right hand curves) and traction/braking forces. All the damage from these different running conditions is superimposed on the wheel tread and cannot easily be related to specific route sections or running conditions. The overall damage rates on the wheel are therefore much more sensitive to the relative rates of wear and crack growth.

To assist in this calibration exercise the following parameters have been investigated:

- Distribution of $T\gamma$ across the wheel (scaled and un-scaled by the directions of the longitudinal creep force) and comparison with the distribution and severity of the observed damage.
- Growth rate of wear and crack damage as a non-linear function of $T\gamma$.
- Influence of the direction of the creep forces on the damage rates [3].

These parameters have been used to test alternative $T\gamma$-damage relationships including modifying the gradient and break points of both the crack and wear damage parameters, identified in Figure 4, until acceptable prediction of the observed RCF damage was achieved. A detailed description of the observations from these investigations is included in [3], which includes a comparison of the observed damage types and locations with the predicted wheel/rail contact parameters and forces.

Figure 13 includes example plots of the distribution of $T\gamma$ across the wheel for powered axles of a typical DMU vehicle. Figure 13(a) illustrates the raw $T\gamma$ and Figure 13(b) the $T\gamma$ scaled by the direction of the longitudinal creep force, such that RCF damage only occurs when the wheel is the driven surface (i.e. braking direction).

In these plots the level of $T\gamma$ is defined on the y-axis and the position across the tread of the wheel on the x-axis (with zero being the flangeback of the wheel). The distribution of contacts at a particular location on the wheel and $T\gamma$ level is indicated by the intensity of the contour scale. The following observations can be drawn from these plots:

- It can be seen from the distribution of the raw $T\gamma$, included in Figure 13(a), that a number of contacts are predicted on the field side of the wheel at the location of the primary band of RCF cracks observed on a large number of fleets (i.e. 80-100mm from the flangeback). These contacts generally have $T\gamma$ values in the range 0-200N and are associated with running on the low rail in curves.
- At the centre of the tread (i.e. 70mm from the flangeback) a large proportion of contacts are predicted with values of $T\gamma$ in the range 0-20N, generally associated with running on straight track resulting in the generation of mild wear rather than RCF damage.
- As expected a large proportion of high $T\gamma$ values are predicted towards the flange of the wheel associated with running in high rail flange contact. The longitudinal forces at these contacts are generally in the traction direction, resulting in the generation of wheel and rail wear, but RCF damage on the rail only. Therefore to ensure the model does not over predict the level of damage in these regions it is appropriate to scale the $T\gamma$ outputs. The influence of scaling the $T\gamma$ by the longitudinal creep force can be seen in Figure 13(b), where the majority of damaging contacts in this region disappear.

- Following scaling of the $T\gamma$ by the direction of the longitudinal creep force, illustrated in Figure 13(b), the majority of damaging contacts in the primary RCF band remain with a value of $T\gamma$ in the range 0-150N. There is also a small proportion of damaging contacts predicted with lower values of $T\gamma$ towards the flange root of the wheel at the location of the secondary band of wheel RCF observed on some fleets (i.e. 50-60mm from the flangeback). This is generated from the trailing wheelset running on the high rail in curves. This type of damage was not observed on the fleets analysed, where the majority of RCF damage was observed in the primary RCF band, and therefore suggests that the dominant damage mechanism for these fleets at this location is wear.

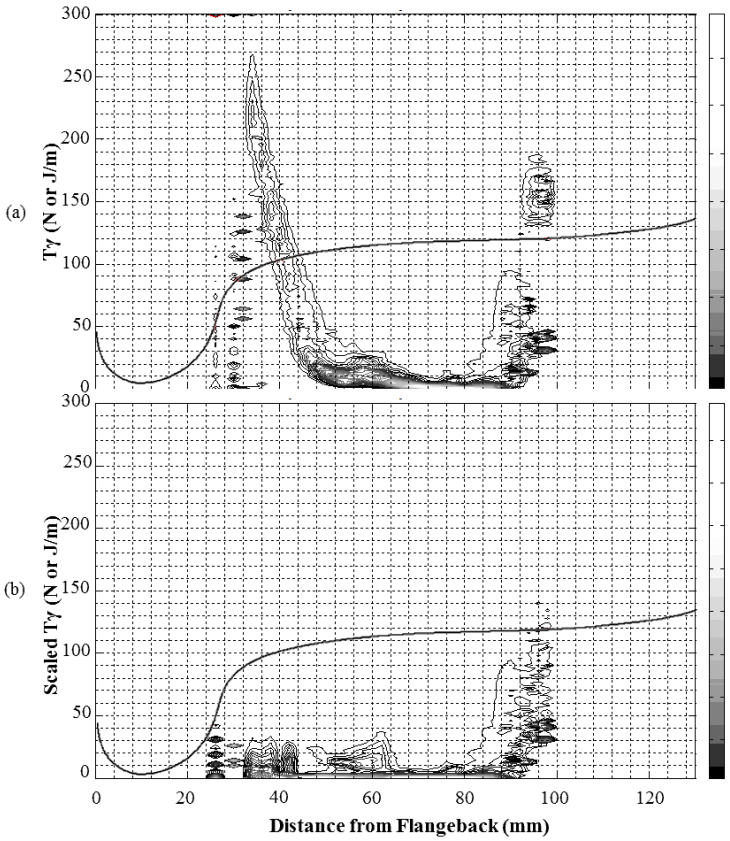

Figure 13 Distribution of Raw $T\gamma$ (a) and Scaled $T\gamma$ (b)

The result obtained from these comparisons have suggested that regions of observed wheel RCF damage typically correlate with the areas of $T\gamma$ (75N < $T\gamma$ < 175N) higher than those associated with the generation of rail RCF (where peak damage occurs at $T\gamma$ = 65N, beyond this value wear increases to counteract the initiation and propagation of RCF). Therefore the peak of the damage function for wheel RCF should occur at a higher value of $T\gamma$. Also, wheel RCF observed on the field side of the wheel is generally caused by forces in the braking direction, usually generated whilst running on the low rail in moderate to sharp radius curves.

Following this calibration exercise it was concluded that the $T\gamma$–wear relationship developed by BR Research [14] provided the best approximation of the depth of wear generated to remove RCF damage. A separate $T\gamma$-crack damage relationship was calibrated to predict the depth of RCF cracks, with the summation of these two parameters providing a measure of the RCF propensity which includes the interaction of wear and fatigue.

4.2.1 Predicted and Observed RCF Damage

The developed $T\gamma$-damage relationships have been validated against observations of wheel RCF damage from a number of GB fleets. This data included considerable variability and scatter due to the influence of numerous factors (e.g. vehicle/route characteristics, material flaws and other damage modes such as wheel flats etc.) and the accuracy of wheel damage observations [2]. Therefore the average of the observed maximum crack lengths has been calculated for each vehicle fleet, separating motor/trailer axles and leading axles of the train where applicable. These have been compared to the outputs from the model by converting the predicted damage depth to a surface crack length (assuming that the modelled crack depth is a quarter of the observed surface crack length).

A linear regression has been fitted to both the observed and predicted average crack length data to allow a numerical comparison between the different vehicle types. The gradient of the linear regression is shown in each of the plots for both the observed and predicted damage and an error bar has been added to the observed average of the maximum crack lengths to indicate the level of scatter in the data. Figure 14 illustrates the observed and predicted crack lengths on the motor and trailer axles of both a typical DMU and EMU vehicle.

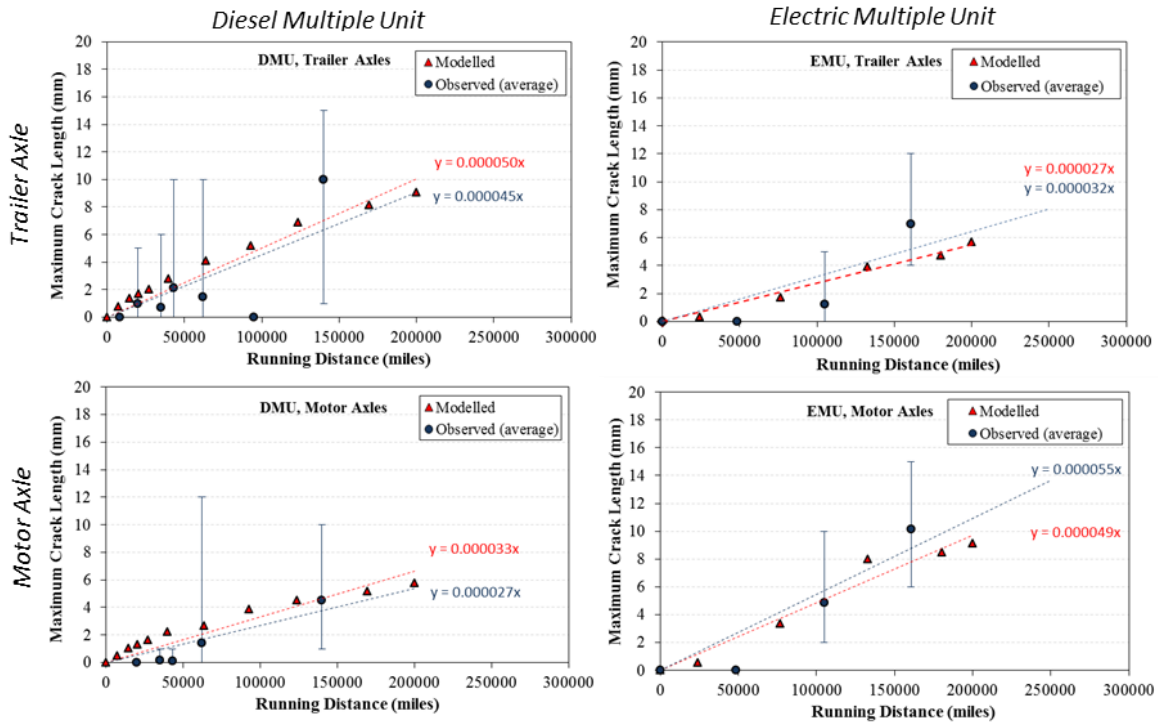

Figure 14 Observed and Modelled Crack Lengths

Generally a good agreement between the modelled and observed damage rates is obtained. This can be seen from comparing the gradients of the linear trend lines, with errors of less than 20%. In all the cases studied the predicted damage rates were within the scatter band of the observed data. The model also predicts the relative damage rates observed between different vehicles and axles.

The data presented in Figure 14 also highlights the differences in wheel RCF damage rates observed between motor and trailer axles on EMU and DMU vehicles. DMU vehicles showed a faster growth rate on trailer axles than motor axles, whereas on EMU vehicles the reverse was true. This is due to the distribution of traction and

braking through the vehicle; on DMU vehicles braking is generally split evenly between motor and trailer axles, while motor axles will exhibit additional wear from traction forces and therefore a lower RCF damage rate. On modern EMU vehicles the majority of braking is applied on the motor axles resulting in higher RCF damage rates, whereas the trailer axles are largely unaffected by the traction and braking forces. This difference is also captured in the modelled damage and illustrates the influence of traction and braking forces on the formation of wheel RCF damage.

The gradient of the linear regression fitted to both the observed and modelled average crack lengths have been determined for all the vehicle types analysed. These values represent the observed and modelled damage rates, in mm per million miles (mm/Mmiles) for ease of presentation, and are compared in Figure 15. The dashed line in Figure 15 indicates a perfect correlation between the predicted and observed damage rates, therefore the closer the data point to this line the better the prediction. Generally it can be seen from Figure 15 that a reasonable correlation is obtained between the modelled and observed damage rates. Fitting a linear regression to this data results in a correlation coefficient of (R^2) of approximately 0.8. This implies that the modelled damage rates are a good correlation with the observed damage rates.

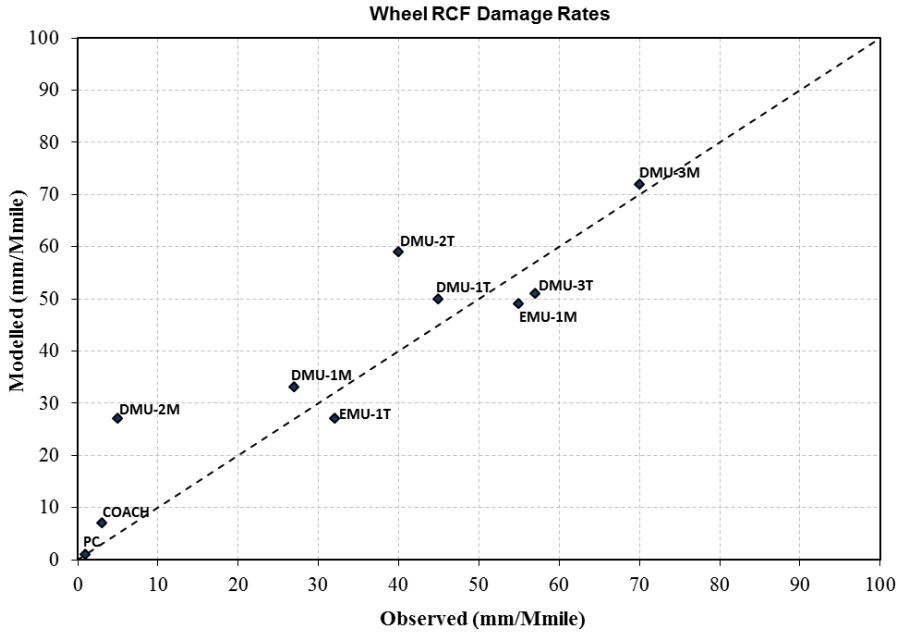

Figure 15 Comparison of Predicted and Observed Damage Rates (T = Trailer, M = Motor)

As discussed above, the damage rates can be significantly influenced by traction and braking, friction coefficients, operating conditions and wheel-rail profiles. Although every effort has been made to ensure that reliable input data is obtained, in many cases this information is not known in details and therefore assumption have been made during the modelling of certain fleets to generate the prediction presented in Figure 15. This might explain some of the different between the modelled and observed damage rates and if more accurate information was made available it might be possible to obtain a better match between the predicted and observed damage rates.

In addition to the average crack lengths, the location (e.g. distance from the flangeback of the wheel and length of the crack) of the RCF damage across the wheel tread was also determined from the observation data. Using this information the proportion of wheels with RCF damage on a particular region of the wheel was determined

and compared to the modelled distribution of damage across the wheel tread. This comparison is illustrated in Figure 16 and has been used to validate the location of the modelled damage (e.g. distance from the flangeback, as illustrated on the x-axis) rather than the actual magnitude of the distribution. For this reason the y-axis on Figure 16 includes a nominal scale, as the units of the observed and modelled distributions are different

It can be seen from Figure 16 that there is a reasonable agreement between the locations of the modelled and observed wheel RCF damage across the wheel tread. For all vehicle types the majority of damage is modelled and observed in a band 70-100mm from the flangeback. Discrepancies in the modelled distributions are possibly associated with the assumptions on rail profiles and track irregularities (lateral alignment and gauge variation) adopted within the model, as the vehicle will generally see a wider variation of rail profiles and track irregularities than included in the simulations.

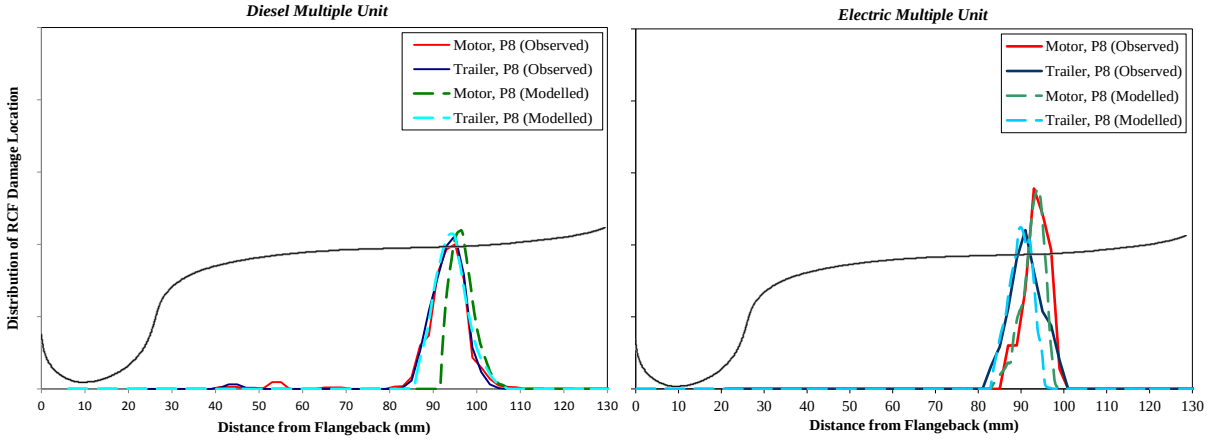

Figure 16 Observed and Modelled RCF Damage Distribution

5. CONCLUSIONS

A model has been developed to predict the rate of wear and rolling contact fatigue (RCF) on the wheel. To assist in the development of the model wheel turning data and observations were analysed to provide information on the actual incidence of different wheel damage modes. Wheel wear and RCF were highlighted as the two main damage modes seen by the wheel that can accurately be incorporated into a wheel damage model. Investigations conducted using the observation data highlighted the sensitivity of the model to a number of input parameters: such as the influence of traction and braking and the different operating conditions of the vehicle.

To capture the variation in running conditions seen by the wheel the model uses a description of a fleet's route diagram to characterise the duty cycle of the wheel in terms of curve radius, cant deficiency and traction/braking performance. Using this duty cycle a number of vehicle dynamics simulations are automatically conducted to calculate the wheel-rail contact forces. The predicted wheel-rail forces are then post-processed to predict the formation of wear and RCF damage on the wheel using a combination of the Archard model (wear) and a $T\gamma$-damage (RCF) relationship. The developed wheel RCF $T\gamma$-damage relationship includes the interaction between wear and crack damage, such that wear reduces the formation of RCF damage.

To assist in the calibration of the RCF $T\gamma$-damage relationship the observed damage types and locations were compared with the predicted wheel/rail contact parameters and forces. These comparisons suggested that regions of observed wheel RCF damage typically correlate with the areas of high $T\gamma$ ($75N < T\gamma < 175N$) and

were generally associated with wheel/rail forces in the braking direction, usually generated whilst running on the low rail in moderate to sharp radius curves.

The rates of wear (tread and flange wear) and RCF damage (crack depth), along with the location of damage on the tread of the wheel, have been compared to the damage observed on a number of fleets in Great Britain (GB). This has resulted in the development of a wheel RCF damage relationship which generally provides good agreement with the observed damage rates for the fleets analysed. The predicted damage rates have been successfully used in the recently developed Wheelset Management Model (WMM) [24, 25] to estimate the emerging wheelset maintenance and renewal costs.

The sensitivity of a number of the input parameters to the model has been investigated using fleet observation data. These investigations highlighted that further analysis is required to understand the influence of certain parameters on wheel damage, these include: traction and braking, performance of wheel slide protection systems and influence of wheel size on damage. Further work is also required to understand the influence of variations in wheel metallurgy (in particular the change in properties through the depth of the wheel rim and service life of the wheelset) and the performance of different wheel steels. Current research work been conducted at the Institute of Railway Research (University of Huddersfield) is investigating a number of these areas [26] with the aim of improving current engineering models and the optimisation of wheelset monitoring and maintenance regimes, thereby reducing whole life costs.

6. ACKNOWLEDGEMENTS

The results and findings included within this paper were developed from the RSSB managed rail industry research programme, funded by the Department for Transport, to increase the rolling stock functionality of the VTISM (Vehicle Track Interaction Strategic Model) tool through the development of a Wheelset Management Model [24, 25].

The GB Vehicle Track System Interface Committee (V/T SIC) and the train operating companies/vehicle maintainers who supplied data to develop and validate the model are also acknowledged for their support during the research work. The authors would also like to thank Mats Berg and Roger Enblom from KTH, Sweden for their contribution to the early stages of this research.

REFERENCES

[1] A. Bevan, S. Iwnicki, Review of wheel turning data and identification of other wheel damage modes, T792 project report, RSSB, 2010.

[2] P. Molyneux-Berry, Wheel RCF – Assessment of fleet observations, T792-01 project report, RSSB, 2011.

[3] P. Molyneux-Berry, A. Bevan, Wheel surface damage: relating the position and angle of forces to the observed damage patterns, Vehicle System Dynamics Supplement, Vol. 50, pp.335-347, 2012.

[4] S. Bogdański, P. Lewicki, 3D model of liquid entrapment mechanism for rolling contact fatigue cracks in rails, Wear, Vol.265, pp.1365-1362, 2008.

[5] J. Nielsen and A. Johansson, Out-of-round railway wheels: A literature survey, Journal of Rail and Rapid Transit (Part F), Vol. 214, 2000.

[6] J. Jergeus, C. Odenmarck, R. Lunden, P. Sotkovszki, B. Karlsson, P. Gullers, Fullscale railway wheel flat experiments, Journal of Rail and Rapid Transit (Part F), Vol.213, 1999.

[7] A. Bevan, Development of a wheel profile damage model, T792-02 project report, RSSB, 2011.

[8] J. Tunna, J. Sinclair, J. Perez, A review of wheel wear and rolling contact fatigue, Journal of Rail and Rapid Transit (Part F), IMechE, Vol. 221, pp.271-289, 2007.
[9] T. Jendel, Prediction of wheel profile wear – Comparison with field measurements, Wear, Vol. 253, pp. 89-99, 2002.
[10] R. Enblom, M. Berg, Simulation of railway wheel profile development due to wear – Influence of disc braking and contact environment, Wear, Vol. 258, pp. 1055-1063, 2004.
[11] T. Jendel, Prediction of wheel profile wear – methodology and verification, Licentiate Thesis, TRITA – FKT 2000:49, Department of Vehicle Engineering, Royal Institute of Technology (KTH), Stockholm, 2000.
[12] R. Enblom, Deterioration mechanisms in the wheel-rail interface with focus on wear prediction: a literature review, Vehicle System Dynamics, Vol. 47, pp.661-700, 2009.
[13] T.G. Pearce and N.D Sherratt, Prediction of wheel profile wear, Wear, Vol. 144, pp. 343-351, 1991.
[14] I. McEwen, R. Harvey, Interpretation of wheel/rail wear number, Report Ref: TM VDY 004, British Rail Research, 1986.
[15] J.F. Archard, Contact and rubbing of flat surfaces, Journal of Applied Physics, Vol.24, pp.981-988, 1953.
[16] A. Bevan, P. Allen, S. Iwnicki, Development of an anti-RCF wheel profile, T547 project report, RSSB, 2005.
[17] A. Bevan, P. Allen, R. Enblom, Application of a wear prediction method to the analysis of a new UK wheel profile, Proceedings of the 7th Contact Mechanics and Wear of Rail/Wheel Systems Conference, 2007.
[18] T, Jendel, M. Berg, Prediction of wheel profile wear, Vehicle System Dynamics Supplement, Vol. 37, pp. 502-513, 2002.
[19] R. Lewis, U. Olofsson, Mapping rail wear regimes and transitions, Wear, Vol. 257, pp. 721-729 2004..
[20] BS 5892-2:1992, Railway rolling stock materials – Specification for monobloc wheels.
[21] A. Ekberg, E. Kabo, H. Andersson, An engineering model for prediction of rolling contact fatigue of railway wheels, Fatigue and Fracture of Engineering Materials and Structures, Vol. 25, pp. 899-909, 2002.
[22] M. Burstow, Whole life rail model application and development – Continued development of an RCF damage parameter, T115 project report, RSSB, 2004.
[23] F. Flanklin, A. Kapoor, A modelling wear and crack initiation in rails, Journal of Rail and Rapid Transit (Part F), IMechE, Vol. 221, pp.23-33, 2007.
[24] D. Ling, A. Bevan, A. Rhodes, Improving the rail industry's VTISM to include wheelset management modelling, Proc. of the Asset Management Conference, IET, London, 2011.
[25] A. Bevan, P. Molyneux-Berry, S. Mills, A. Rhodes and D. Ling, Optimisation of wheelset maintenance using whole system cost modelling, Proceedings of the Institution of Mechanical Engineers, Part F: Journal of Rail and Rapid Transit, 2013.
[26] P. Molyneux-Berry, A. Bevan, The influence of wheel/rail contact forces on the material properties of wheels in service, Proc. of 9th International Conference on Contact Mechanics and Wear of Rail/Wheel Systems (CM2012), China, 2012.

NOMENCLATURE

DMU Diesel Multiple Unit
GB Great Britain
RCF Rolling contact fatigue
WMM Wheelset management model
VTISM Vehicle track interaction strategic model
RCF_{grad} Slope of modelled RCF damage
RCF_{thres} Mileage threshold for RCF_{grad}
Sh Flange height
Sd Flange thickness
Sd_{grad} Slope of modelled flange thickness
Sh_{grad} Slope of modelled flange height

Sh_{thres}	Mileage threshold for Sh_{grad}
Vw	Material loss
N	Normal force
s	Sliding distance
H	Material hardness
v_{slip}	Slip velocity
p	Contact pressure
$T\gamma$	Frictional energy dissipated in the contact patch, expressed as the sum of the products of the creepage and creep force for the lateral, longitudinal and spin components
T_y, T_x	Longitudinal and lateral creep force
M_z	Spin creep moment
γ_y, γ_x	Longitudinal and lateral creepage
ω_z	Spin creepage